INCLUSIVE PUBLISHING
TRUSTED SCIENCE

4D printing and annealing of PETG composites reinforced with short carbon fibers

To cite this article before publication: Davood Rahmatabadi *et al* 2024 *Phys. Scr*. in press https://doi.org/10.1088/1402-4896/ad3b40

View the article online for updates and enhancements.

4D Printing and Annealing of PETG Composites Reinforced with Short Carbon Fibers

Davood Rahmatabadi[a], Elyas Soleyman[a], Mahshid Fallah Min Bashi[a], Mohammad Aberoumand[a], Kianoosh Soltanmohammadi[a], Ismaeil Ghasemi[b], Majid Baniassadi[a], Karen Abrinia[a], Mahdi Bodaghi[c*] and Mostafa Baghani[a*]

[a]*School of Mechanical Engineering, College of Engineering, University of Tehran, Tehran, Iran*
[b]*Faculty of Processing, Iran Polymer and Petrochemical Institute, Tehran, Iran*
[c]*Department of Engineering, School of Science and Technology, Nottingham Trent University, Nottingham NG11 8NS, UK*

[*]Corresponding authors: mahdi.bodaghi@ntu.ac.uk; baghani@ut.ac.ir

Abstract

In this study, for the first time, post-heat treatment was applied to improve the stress recovery of short carbon fiber reinforced PETG (SCFRPETG). PETG and SCFRPETG composite were printed under optimal conditions, and constrained and free shape memory cycles were applied under compression and three-point bending loadings to assess shape and stress recovery. The results of the free shape memory test for both vertical and horizontal patterns showed that PETG composite also has a higher shape memory effect (SME) compared to PETG. The SME was significantly improved by performing heat treatment. The stress recovery values for pure PETG, reinforced PETG before and after annealing are 2.48 MPa, 3.04 MPa and 3.18 MPa, respectively. It shows that the addition of 1.5% carbon fiber increases the stress recovery by 22%. The increasing trend reaches 28% by performing post-heat treatment. Additionally, altering the printing pattern affects the programming and stress recovery values. For the SCFRPETG composite samples before and after annealing, changing the printing pattern from horizontal to vertical, resulted in a 16% and 7% increase in recovery stress, respectively. SEM results confirm that the annealing process removes the layered structure, micro-holes caused by shrinkage and 4D printing mechanism. Using the controlled heat treatment method can be a practical solution to solve the problem of adhesion and reduce the anisotropy of FDM 3D printed layers.

Keywords: PETG; Short carbon fiber; 4D printing; Annealing; shape memory effect

1- Introduction

1

One of the most rapidly expanding technologies for producing components through rapid prototype methods is additive manufacturing (AM) [1]. In this method, a part is printed layer-by-layer, simplifying the production of detailed and complex geometries [2,3]. Another impressive advantage of this type of fabrication is the significantly low amount of waste generated during the process compared to other manufacturing methods [4,5].

3D printed parts have relatively lower mechanical properties compared to traditional manufacturing methods. In one of the 3D printing methods, thermoplastic polymers can be used as feedstock, known as Fused Deposition Modeling (FDM) [6]. FDM is the most widespread technique with the most economical price for printing a 3D part using AM [7,8]. Permanence, ease of use, wide availability, simple feedstock, and significantly lower initial investment compared to other manufacturing methods are the additional benefits that make it one of the most preferred fabrication methods in various industries [4,9]. PLA and ABS are the most commonly used materials in FDM [10]. In addition to them, other materials such as PETG, polycarbonate, and nylon are also of great interest and use. PETG is derived from polyethylene terephthalate (PET) that combines with a glycol group to the polymeric chain and achieves new properties [11,12]. The presence of glycol results in better flowability and a lower glass transition temperature, making it more suitable for use in 3D printing processes [11,12]. Additionally, lower cost and higher strength compared to other polymers are other main reasons for using PETG in the FDM method [11,12]. Another interesting trait of PETG is its Shape Memory Effect (SME) which allows it automatically recover its deformed shape by changing the temperature. The combination of this SME and the good printability of PETG make it a suitable choice for use as the feedstock in 4D printing [13,14]. The 4D printing process involves combining AM methods like FDM, with smart materials such as PETG, which is a shape memory polymer (SMP). This extra dimension in 4D printing allows for

2

dynamic attributes over time, resulting in novel abilities in 3D printing such as actuation, self-adaption, self-assembly, and perception [11]. Soleyman et al. studied the tensile shape memory and self-coiling behavior of 3D-printed PETG parts. The results showed that hot-programmed samples had an excellent shape fixity ratio above 99%, while their shape recovery ratios were 40-60% [13]. Aberoumand et al. studied the shape recovery performance of PVC 4D printed parts under 3-point bending and compression modes (free recovery tests). The study showed that a higher deformation temperature results in a higher shape fixity ratio but lower shape recovery [15]. The SMPs with high stress recovery are necessary for actuator and self-healing applications. However, the amount of recovery stresses in SMPs typically ranges from tenths to several MPa which is not ideal for industrial applications [16,17].

Some research focused on increasing the stress recovery of SMPs. Poulin et al. demonstrated a polyvinyl alcohol (PVA)-carbon nanotubes (CNTs) nanocomposites fiber with a remarkably high stress recovery (~150 MPa) [18]. Increasing stress recovery typically requires increasing strength. As mentioned, the 3D printed parts exhibit low mechanical properties which is a significant issue. To enable widespread applications of this method, optimizing mechanical properties such as strength and toughness is necessary [14]. Various techniques such as fiber-reinforced polymers, optimizing printing parameters, printing in an oxygen-free environment, and annealing have been used to improve mechanical properties [19,20]. Mohammadizadeh et al. studied the mechanical and structural properties of Continuous Fiber Reinforced Additively Manufactured components, showing that the presence of these reinforced fibers in the structure, results in superior mechanical properties compared to other specimens [21]. Even though continuous fiber composites offer significant mechanical performance improvements, they are not commonly used material in processing, unlike short-fiber reinforced polymers (SFRP) [22]. SFRP composites can achieve

3

comparable stiffness levels to continuous fibers while still maintaining the ability to form complex shapes like unreinforced polymers [23]. To enhance the mechanical and thermal properties of PETG filaments, common reinforcements such as short carbon fiber, carbon nanotubes, and glass fiber can be incorporated into the structure. PETG with added carbon fiber (CFPETG), demonstrates a strength increase of 10-25% compared to un-reinforced filament. Another benefit of adding carbon fiber is the enhancement in modulus of elasticity in all printing orientations [24]. Tekinalp et al. conducted a study on the impact of carbon fiber reinforcement on the tensile strength and young's modulus of the ABS copolymer (GP35-ABS-NT). The study revealed that factors such as fiber length, orientation, and porosity influence mechanical properties. The strength of a test piece (52.9 kN.m/kg) with reduced porosity through carbon fiber reinforcement surpass that of Aluminum 6061-0 (45.9 kN.m/kg) [22]. Also, optimizing the FDM process parameters such as layer thickness, nozzle diameter, flow rate, deposition speed, and temperature conditions will cause better mechanical properties in FDM parts [25]. Syrlybayer et al. wrote a review of the influence of the printing parameters on the strength properties of FDM printed parts. According to this review, fusion between two layers occurs before cooling down the extruder below its glass transition temperature, so the longer it is kept at a high temperature, the better the bond will be formed. This is the reason why PLA with lower glass transition temperature and lower heat conduction than ABS, gains better mechanical properties as well because of better fusion in adjacent layers and filaments. In addition, the air gaps in the structure depend on layer thickness which could be controlled by adjusting the nozzle diameter [26].

The other solution to improve the quality of the mechanical properties of the FDM components is annealing [27–29]. This is a post-process that includes heating the material to a high temperature above its glass transition temperature to enhance the chains' molecular mobility in the structure

4

and keeping it at this temperature for a specific time resulting in amplifying interlayer bonding [30]. Shbanah et al. studied the effect of heat treatment (annealing) on the mechanical properties and structure of PLA. They heat-treated the printed specimens at 55°C, 65°C and 80°C for 5 hours and then keeping them at 20 °C for 15 hours. The results of their work show that the optimal heat treatment was 65 °C for 5 hours and also presented a 35% increase in the tensile strength of the material and a decrease in the amount of porosity in the structure [27].

In this work, the effect of annealing heat treatment on the structure of 4D printed PETG parts reinforced with short carbon fiber was investigated. The shape recovery performance of the three items under consideration including normal PETG, the short carbon fiber PETG (SCFPETG), and the annealed SCFPETG was evaluated via free and constrained recovery tests under compression loading. The investigation was conducted for two vertical and horizontal printing patterns. Furthermore, the shape memory cycle (programming and free recovery) was also performed in the three-point bending loading mode.

2- Materials and methods

2.1. Materials and 3D printing

Used materials are two types of commercial PETG and short carbon fiber reinforced PETG (SCFRPETG) thermoplastic filament by YS company. Table 1, shows the optimum conditions for printing the mentioned two types of materials, PETG, and short carbon fiber reinforced PETG that were achieved by proposal of the manufacturer and trial and error. Figure 1 shows the schematic of the FDM process. The compression and bending test samples were printed in two different

5

printing directions (horizontal and vertical) and in dimensions of 20×20×20 mm and 50×10×3 mm, respectively.

Table 1. Printing parameters

Constant printing parameters	PETG	Reinforced PETG
Bed Temperature (°C)	50	80
Layer thickness (mm)	0.2	0.2
Nozzle Temperature (°C)	240	260
Speed (mm/s)	40	40
Nozzle diameter (mm)	0.4	0.4
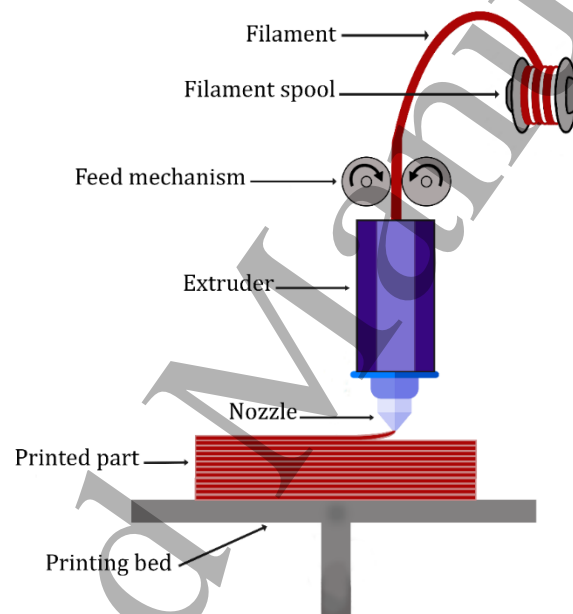
Figure 1. Schematic of the FDM manufacturing process

2.2. Heat treatment operation

The main purpose of this article is to investigate the effect of annealing on the shape memory properties of short carbon reinforced PETG. For this purpose, the heat treatment consists in raising the temperature of the SCFRPETG printed test sample to 120°C, and once the part has reached the target temperature, the temperature was maintained for 3 hours. The material was heated in a metallic mold in a furnace that heats the substance in vacuum conditions.

6

2.3. Programming, Constrained and Free Shape Recovery Protocols

After 3D printing the SCFRPETG samples and applying heat treatment as a post-processing, shape memory properties were evaluated by applying two different recovery protocols (constrained and free) under compression loading. Samples were programmed before constrained and free recovery protocols. Programming also includes four stages of initial heating, loading (applying strain), cooling and unloading. At the end of the programming according to Equation 1, the amount of shape fixity is calculated. The initial heating temperature, heating rate, applied strain, cooling temperature, and cooling rate were considered to be 90°C, 8°C/min, 40%, 25°C, and 15°C/min, respectively. In Figure 2(a), the schematic of the programming under compression loading mode is presented. In Figures 2(b) and 2(c), two different protocols of free and constrained recovery are presented, which respectively specify the two main characteristics of the shape memory effect, i.e. shape recovery and stress recovery. In fact, in the free recovery stage, by heating up to 90°C (8°C/min heating rate), the amount of shape recovery was calculated according to Equation 2. In the same way, the constrained recovery was also conducted by applying restrictions to prevent shape recovery and measuring the force recovery, which is presented schematically in Figure 2(c).

In addition, according to Figure 3, the shape memory cycle (programming and free recovery) was also performed in the three-point bending loading mode. Shape memory tests were repeated on three samples in each loading mode and protocol.

$$\text{shape fixity ratio} = \frac{Remained\ deformation}{Applied\ uniaxialed\ displacement} \times 100 \qquad (1)$$

$$\text{Shape recovery ratio} = \frac{Recovered\ deformation}{Recoverable\ deformation} \times 100 \qquad (2)$$
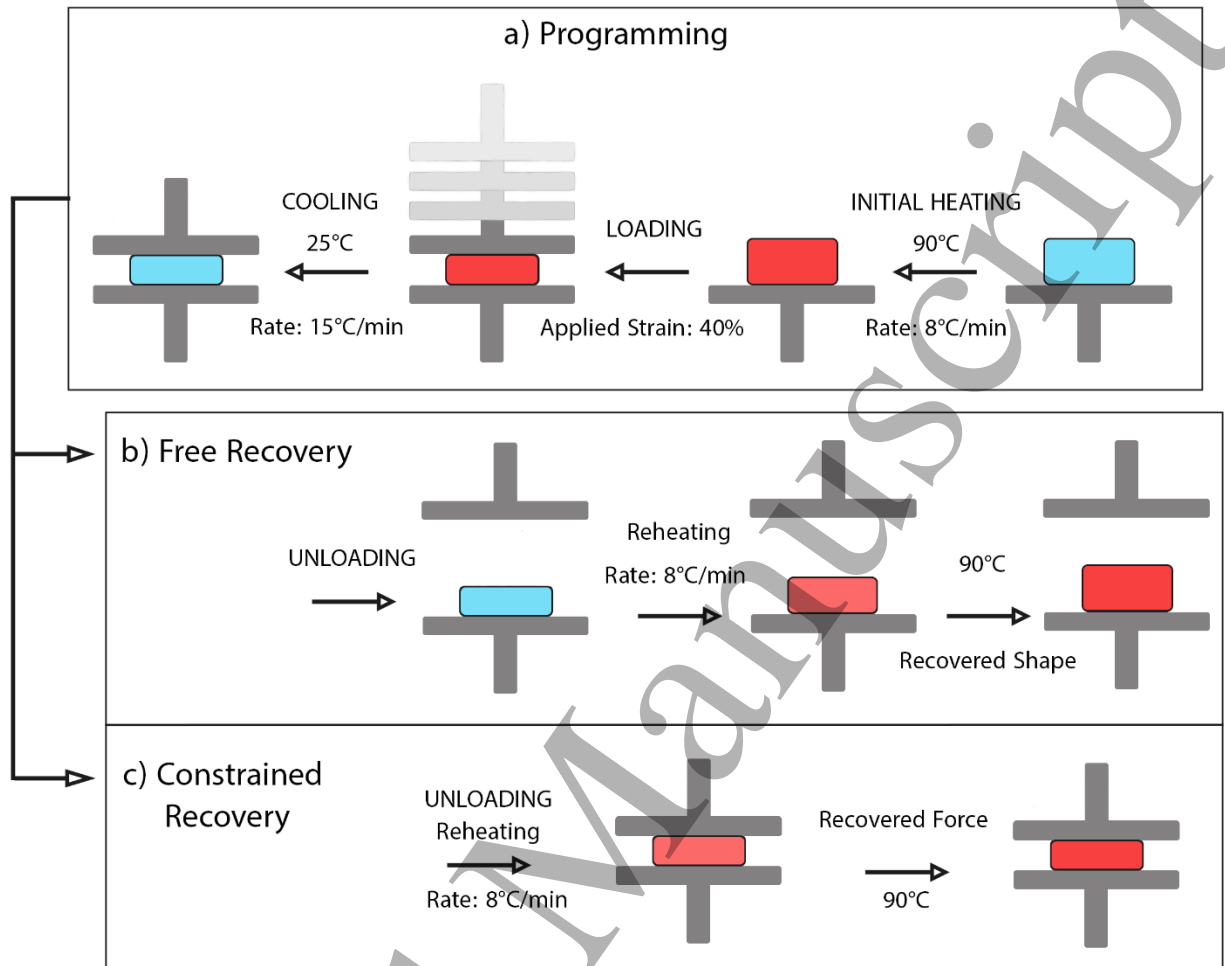
Figure 2. Schematic of the programming two approaches of the recovery stage in shape memory cycle, (a) programming and (b) free shape recovery and (c) constrained shape recovery
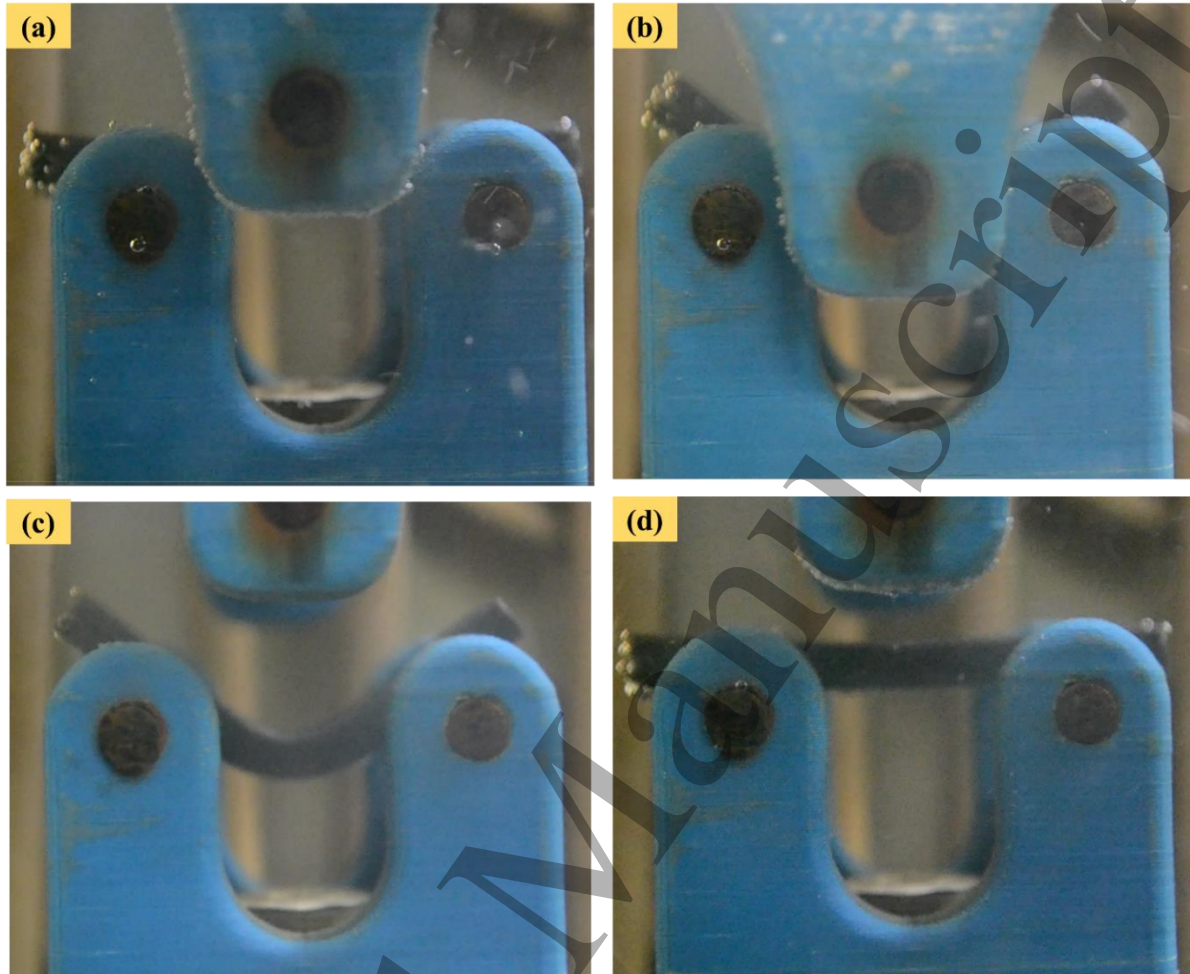
Figure 3. Shape memory cycle under three-point bending mode: (a) heating, (b) loading, (c) cooling and unloading, and (d) reheating and recovery

2.4. SEM

In order to image of the fracture cross-section, 3D printed samples before and after heat treatment were broken down into the liquid nitrogen to have a brittle failure (failure in the glass area), and then, they were coated by gold. Polymers have soft fracture in both transition and rubber regions. For this purpose, in order to prevent soft fracture at ambient temperature and to ensure brittle fracture, the temperature of the sample was reduced to sub-zero temperature by placing it in liquid nitrogen and then it was broken. The quality of the linkage between fibers and matrix, layer junction and rasters, and also the scales of porosities and voids were assessed by SEM.

3. Results and discussion

3.1. Constrained shape memory cycle

The most substantial parameter in SMPs that determine the quality of the shape memory properties

of the material in various applications is the stress recovery. It stems from the generated elastic

recovery stress in the deformation process. Elastic stress is produced and reserved in the SMPs

structure by cooling down the piece after deforming at a high temperature. Reheating the deformed

and fixed SMP above the transition temperature is leading to the release of the stored stress in the

material as the stress recovery. So, shape memory effect is considered a thermomechanical cycle

that includes three stages: stress generation, stress storage, and stress release [11]. In addition, in

hot temperature programming, entropy changes also play a significant role in the recovery process

[15].

The following series of Figures (4-6) show the shape memory cycle and the recovering capability

of the applied stress in three different conditions of the material printed with vertical and horizontal

patterns. First, the ordinary 3D printed PETG, second, the reinforced PETG by short carbon fiber

(SCFPETG), and in the third Figure, the annealed SCFPETG has been examined. In accordance

with Figures 4-6, which apply the shape memory cycle to different samples, it can be seen that at

first the temperature of the samples increases up to 85°C, and then the loading is carried out at a

constant temperature, and as the amount of strain increases, the stress also increases. In the next

step, while the strain is constant, the amount of stress reaches almost zero as the temperature of

the sample decreases to the PETG glass transition range. In fact, changing the structure from rubber

to glass causes polymer chains to freeze and store programming force and entropy. In the ideal

case, this stress reaches zero, which indicates the complete freezing of the force and the deformed

structure. All this process that includes chain stretching in the applied loading direction, quick

10

cooling and maintaining, caused a remarkable reduction in entropy in the thermodynamic system that is the essential driver in shape recovery and stress recovery. In the second stage (recovery stage), as soon as entering the glass transition zone, the recovery of the stress and shape begin due to loosening the restrictions and hard points of the microstructure. In other words, the free volume enhances because of the rise in temperature and the system desires to increase the entropy and approach the thermodynamic equilibrium. For this reason, the areas that have more free volume begin to recover at lower temperatures [11].

Figures 4 (a) and (b) show the constrained shape memory cycle for 3D printed PETG (in vertical and horizontal pattern) due time. In these diagrams, the shape memory cycle that was explained is clear, and quantitative parameters including recovery and programming stress values were extracted for both horizontal and vertical printing patterns. According to Figure 7, the programming stress values for printed PETG with vertical and horizontal patterns are 2.49 MPa and 2.03 MPa, respectively. Therefore, the amount of programming stress for the vertical pattern is 1.23 times more than the horizontal. In the case that the grids and rasters are in the direction of applying force, they show more resistance than when the force is applied in the direction perpendicular to them [31]. This difference is more profound in the stretching mode. In fact, in the vertical pattern, their resistance is higher than when these grids are pressed together, and due to the weaker connection between the grids, this happens with less force, and a part of the initial displacement is used to remove the microholes between the grids and layers. Similarly, the recovery stresses are higher for the vertical pattern than the horizontal.
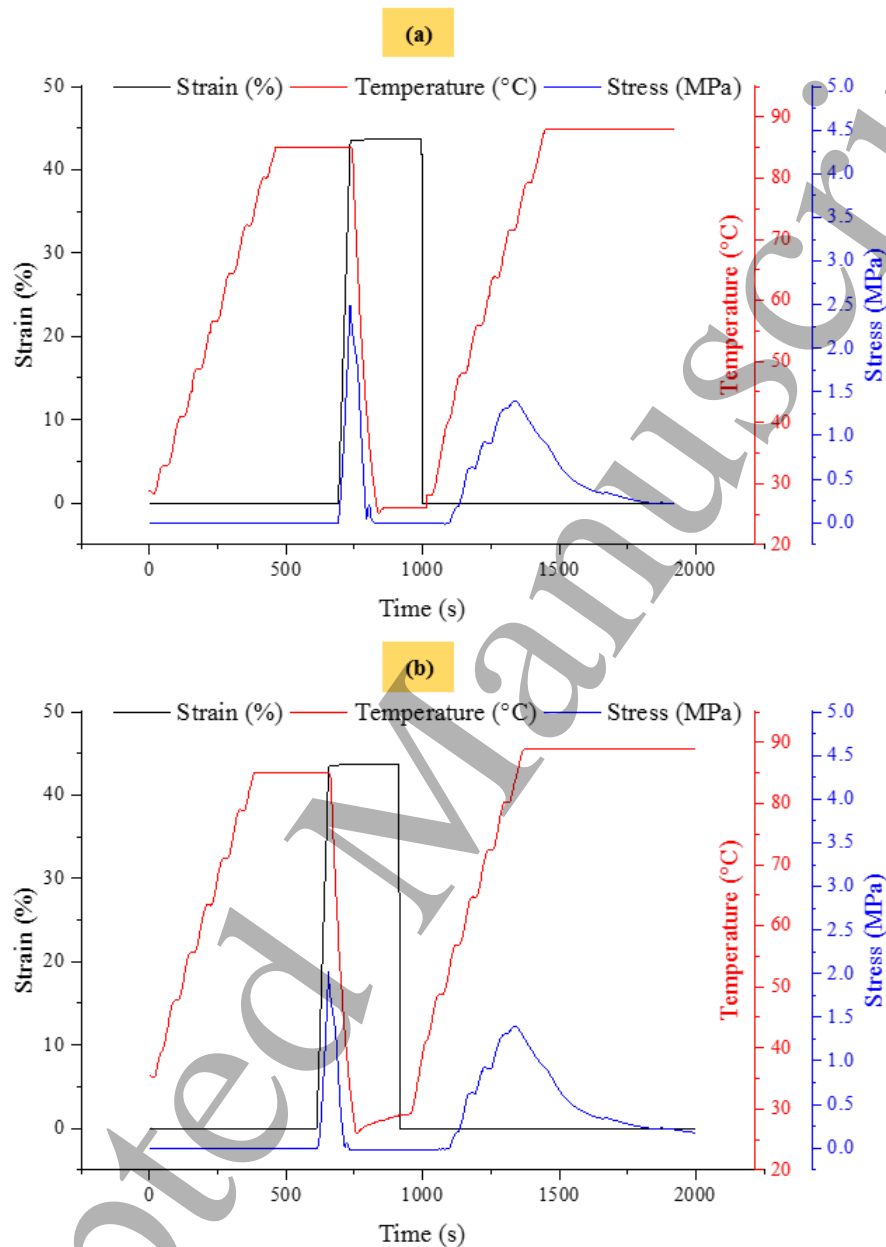
Figure 4. Shape memory cycle for 3D printed PETG via: (a) vertical and (b) horizontal patterns

Moreover, Figures 5 shows the shape memory cycle and the recovery stress of the for 3D printed SCFPETG in (a) vertical and (b) horizontal pattern. As is evident, because of the presence of short carbon fibers in the structure of the polymer, higher loading stress are required to achieve the 40% strain compared to pure PETG. The values of the programming and recovery stress for the

12

composite PETG printed by vertical pattern are 3.04 MPa and 2.06 MPa, respectively, which are improved by 22% and 48% compared to pure PETG. In this case, in addition to the fact that both recovery and programming stress have increased, the value of the stress recovery ratio has also increased. The stress recovery value for the horizontal pattern is also 1.77 MPa, which is more than pure PETG. Therefore, the process of the pattern effect has been preserved for the SCRPETG composite, and the vertical pattern has a higher programming and recovery stress.

13
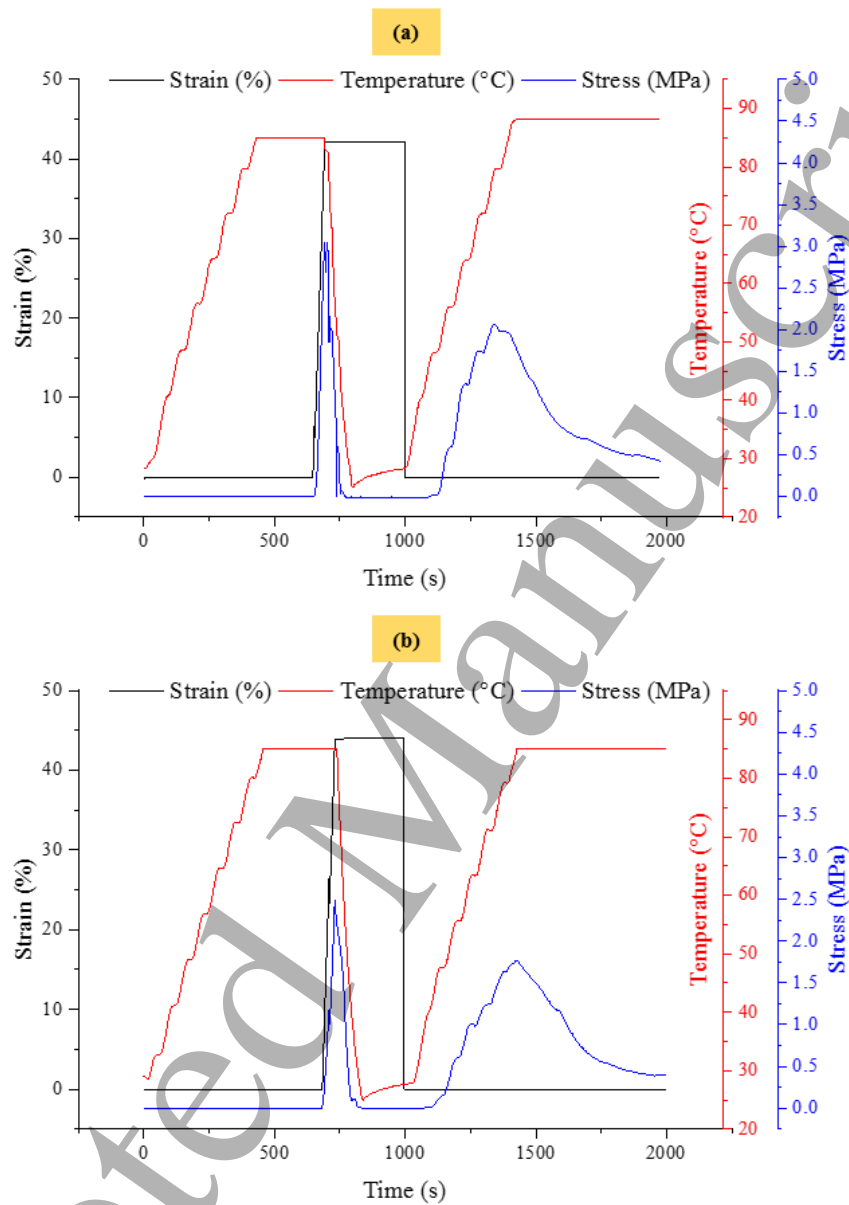
Figure 5. Shape memory cycle for 3D printed SCFPETG via: (a) vertical and (b) horizontal patterns

The process of investigating the stress recovery capability of the 3D-printed SCFPETG after annealing is exhibited in Figure 6. As it shows, we can Figure out that the value of the stress recovery increases in both patterns (vertical and horizontal) compared to the SCFPETG without annealing. In addition, the programming stress values for the annealed composites have been

14

improved. For a more detailed investigation, quantitative parameters were extracted and compared
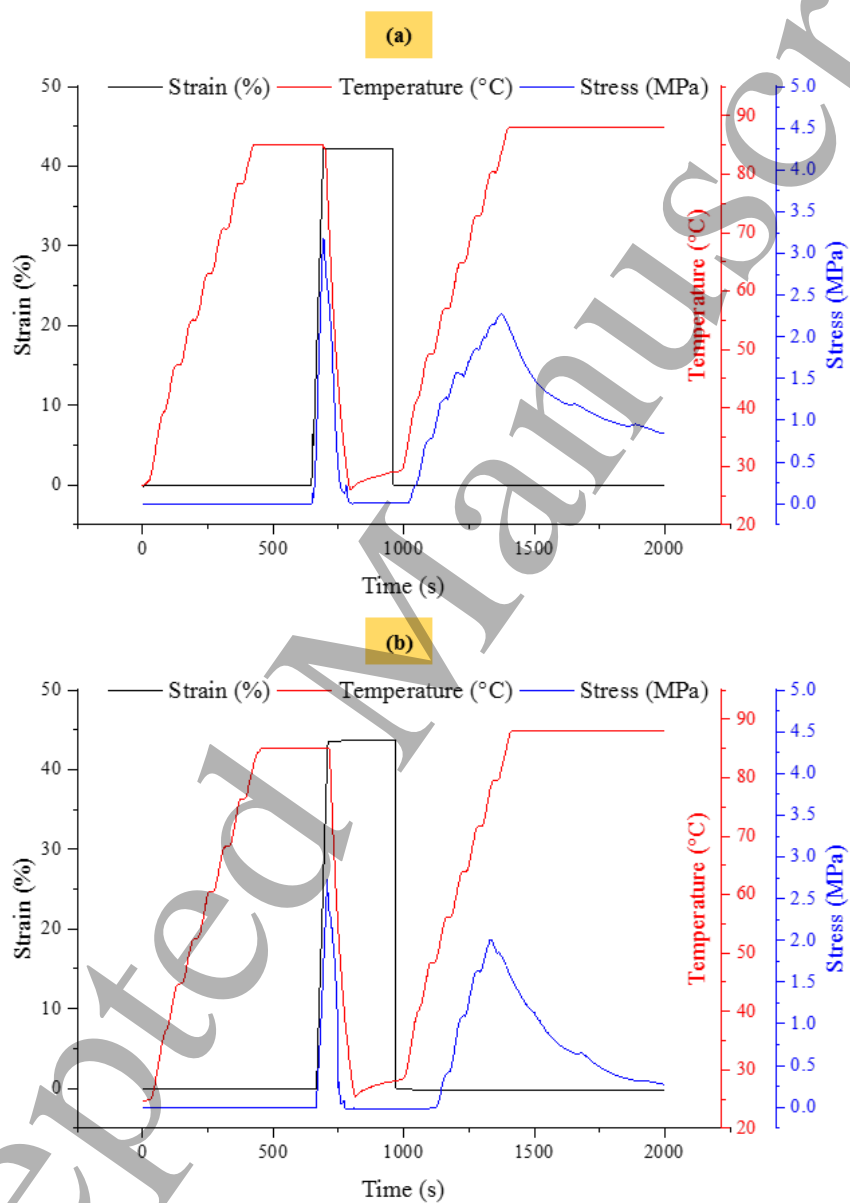
with pure PETG and SCFPETG samples.

Figure 6. Shape memory cycle for 3D printed SCFPETG via: (a) vertical and (b) horizontal patterns after annealing

15

According to the results of Figure 7, the annealed samples show higher programming stress and recovery in both horizontal and vertical patterns. The recovery stress values for pure PETG, reinforced PETG before and after annealing are 2.48 MPa, 3.04 MPa and 3.18 MPa, respectively, which shows that with the addition of 1.5% carbon fiber, the stress recovery increases by 22%. In addition, the increasing trend reaches 28% by performing post-heat treatment. In addition to this, changing the printing pattern also has an effect on the programming and recovery stress values, so that for the SCFRPETG composite samples before and after annealing, by changing the printing pattern from horizontal to vertical, the recovery stress increases by 16% and 13%, respectively.
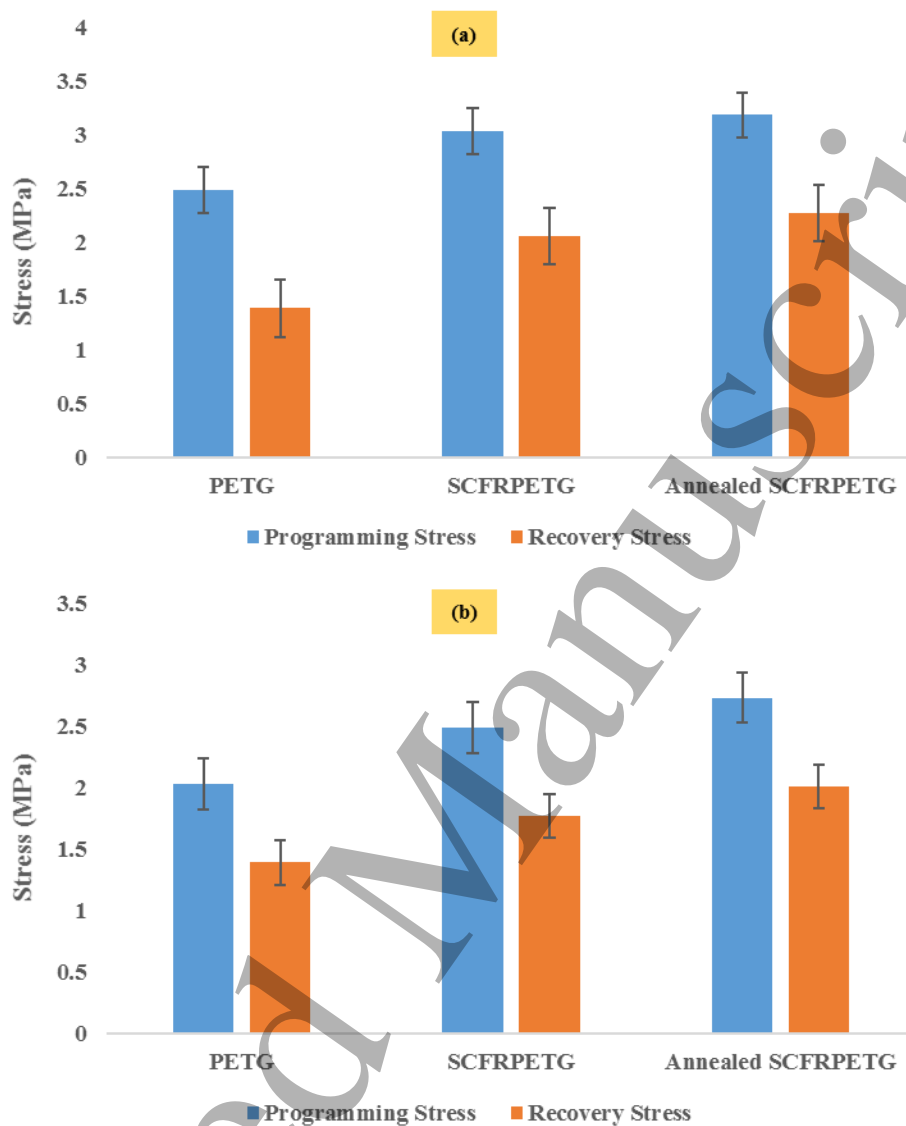
Figure 7. Variations of programming and recovery stress for PETG, SCRPETG and annealed SCRPETG: (a) Vertical and (b) Horizontal patterns

3.2. Free Shape recovery in 3-point bending mode

Figure 8, depicts the ratio of shape recovery and shape fixity of the samples in vertical and horizontal patterns. These charts are presented according to the results of the shape memory cycle test with 3-point bending loading and free recovery. As mentioned in section 2.4, the programming (loading) stage in this approach is the same as the constrained recovery that was described in detail in section 3.1. In this protocol, there is a free recovery stage, where a deformation occurs in the SMP material structure that is meant to be recovered. As shown in Figure 4 and Figure 8, complete shape recovery is obtained the for SCFRPETG samples before and after annealing. Due to the low applied strain in bending mode loading and also the presence of molecular entanglements as network points for SCFRPETG, full shape recovery is achieved. In fact, with the addition of carbon fiber, the elastic part is strengthened and by heating the sample and creating an empty space, recovery is done completely. Of course, the amount of shape recovery for pure PETG is also above 90% in both patterns, which is due to its acceptable shape memory effect, which has already been observed. According to the results of Figure 8, in pure PETG and composite PETG samples, the printing pattern has an effect on the shape fixity values, and as in the previous section, the samples with vertical pattern show better behavior. This dependence is removed in the composite sample after annealing and both patterns show the same shape fixity. The main reason can be the better adhesion of the layers by performing heat treatment and even removing the layered structure.

18
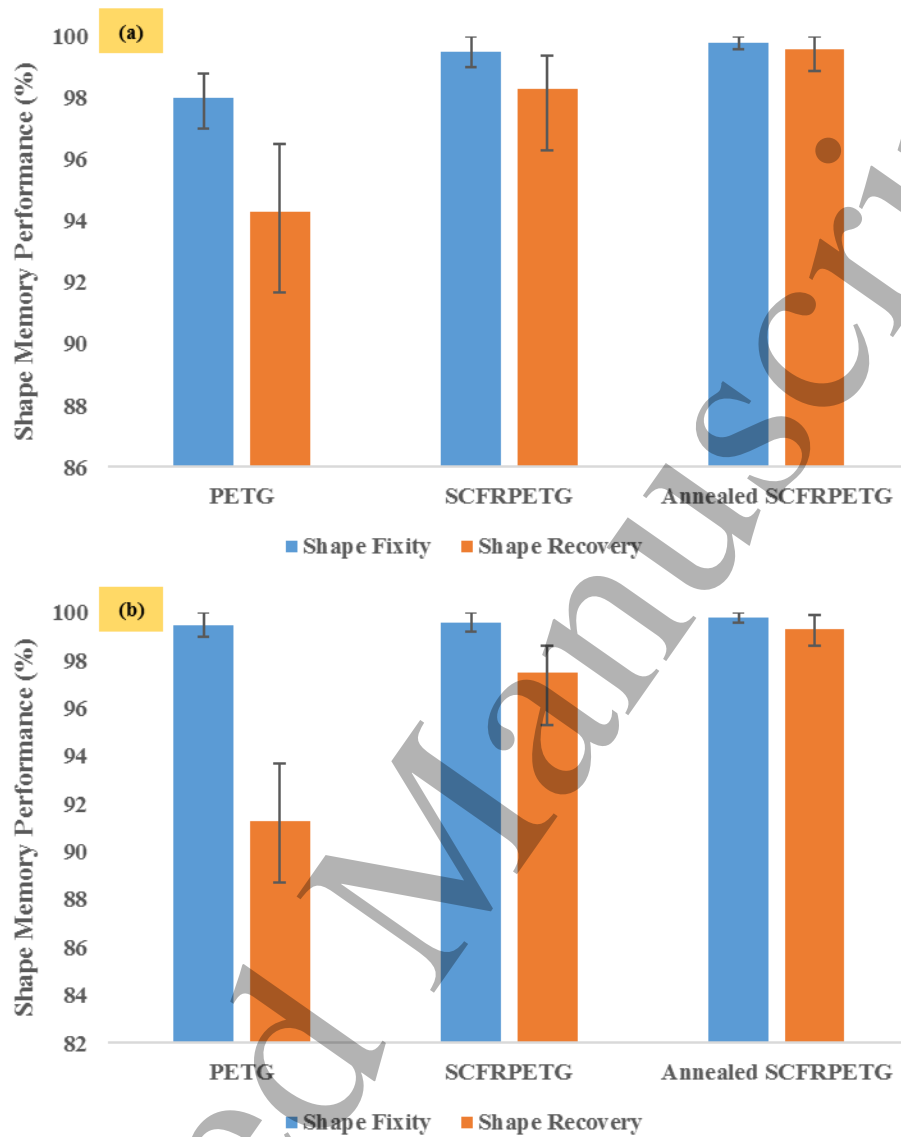
Figure 8. Variations of shape fixity and shape recovery ratio for PETG, SCRPETG and annealed SCRPETG: Vertical and (b) Horizontal patterns

3.3. SEM

In Figure 9, SEM images of 3D printed SCFPETG sample before and after annealing are indicated. Porosity formation in the structure of carbon fiber-reinforced polymers during construction is a considerable issue that affects joint function and adherence [18]. The structure of PETG polymer with 1.5% short carbon fiber (Figure 9, a-c), contains a significant amount of porosity. FDM

feeding mechanism and the contraction of the liquid polymer after cooling are the causes of the establishment of these cavities [32,33]. In addition, in the fiber-reinforced composites, due to the weak fiber-polymer interface, this problem is aggravated, and as seen in Figures 9(a-c), microholes are stretched. It is optimal to reduce them by various solutions such as annealing. According to Figure 9 (d-f), after the annealing operation, the layered structure and stretching the microholes at the interfaces of the grids and layers have been removed, the holes caused by the place of the fibers are observed. As mentioned in the previous section, the annealing operation eliminates the effect of the layered structure and minimizes the effect of the printing pattern on the mechanical properties and shape memory effect. As can be seen, the uniform distribution of short carbon fiber in Figures 9 (e) and (f), can achieve balanced mechanical properties with much less anisotropy. In addition, with the addition of carbon fiber, the resistance of grids against shrinkage increases, and in this way, it helps to improve the microstructure and adhesion of the layers. Strengthening the fiber-polymer interface is another reason for improving microstructural and mechanical properties by annealing. As a result of annealing (Figure 9, d-f), the cohesion between the polymer and the reinforcement carbon fibers are amplified and also the internal voids and porosity are almost disappeared. In general terms, the interfacial adhesion has a direct relation to the mechanical properties of composite [19]. Also, the infill density increases and causes the participation of a higher volume of materials in the recovery stage, and a higher stress recovery is achieved.
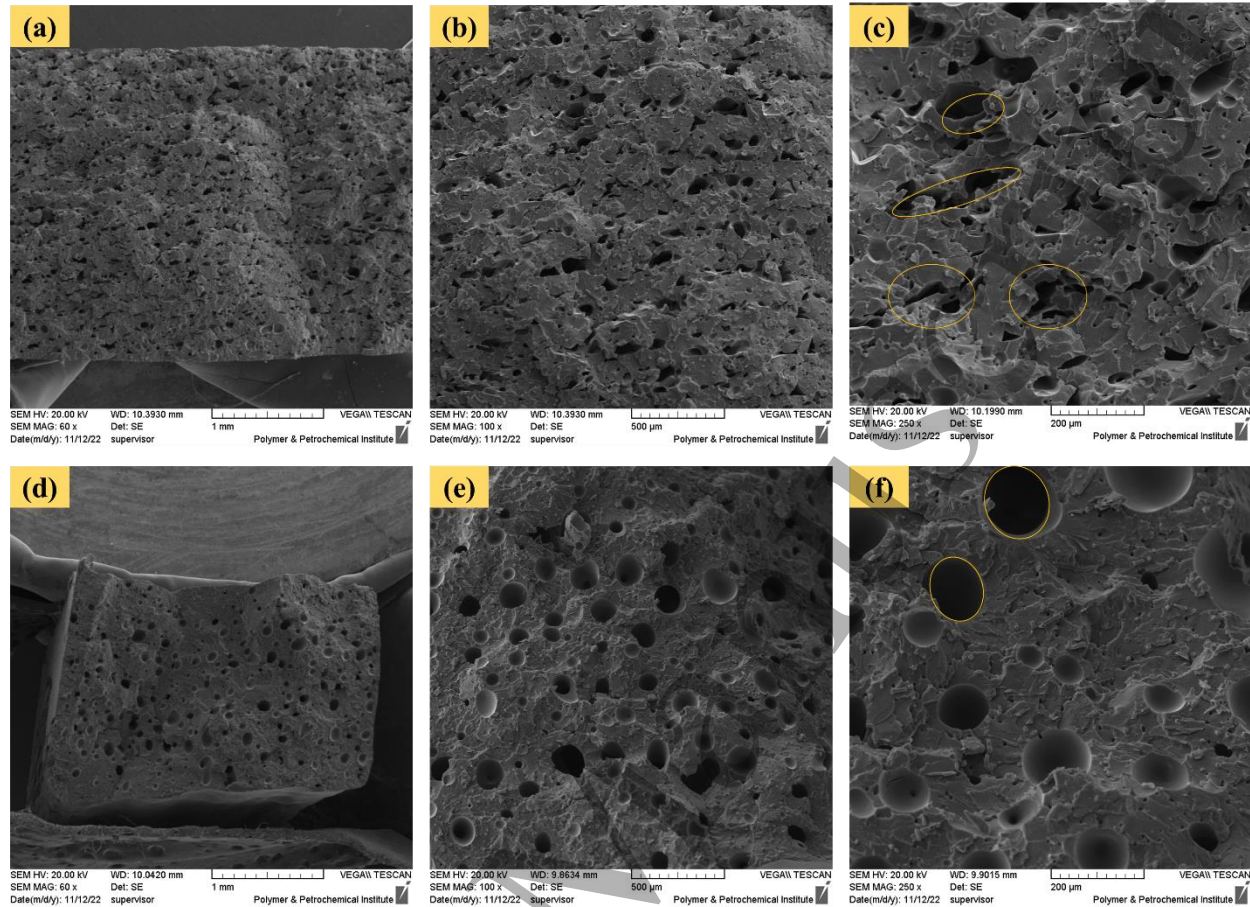
Figure 9. SEM images of: (a-c) 3D printed SCFPETG and (d-f) 3D printed SCFPETG after annealing

4- Conclusion

In this research, for the first time, short carbon reinforcement and heat treatment after 4D printing were used to improve the stress recovery of 3D printed PETG during shape memory cycle. Samples of PETG and SCFPETG were printed with optimal condition and constrained and free shape memory cycles were tested under compression and three-point bending loading modes. In order to investigate the effect of annealing on the mechanical properties of SCFPETG, the printed samples were annealed at 120°C, and was maintained for 3 hours. Eventually, the following results were obtained:

- shape memory effect (SME) was significantly improved by performing heat treatment in both vertical and horizontal patterns. The values of the stress recovery of pure PETG, short carbon reinforced PETG before and after annealing are 2.48 MPa, 3.04 MPa, and 3.18 MPa. These values show that stress recovery increases by 22% with the addition of 1.5% carbon fiber and then increases by 28% by performing post-heat treatment.

- The stress recovery values were higher for the vertical pattern than the horizontal pattern due to the higher resistance caused by grids and rasters being aligned with the direction of applying force. Therefore, changing the printing pattern also had an effect on the programming and recovery stress values. Thus, for the SCFRPETG composite samples before and after annealing, by changing the printing pattern from horizontal to vertical, the stress recovery increases by 16% and 13%, respectively.

- In 3-point bending mode, with the addition of carbon fiber, the elastic part was strengthened and by heating the sample and creating an empty space, the full shape recovery was achieved, while the amount of shape recovery for pure PETG was also above 90% in both patterns.

- In both pure PETG and composite PETG samples, the printing pattern influenced the shape recovery values with samples showcasing vertical patterns demonstrating superior behavior. Following annealing, both patterns displayed complete shape recovery (100%) as a results of enhanced layer adhesion from the heat treatment, effectively eliminating the layered structure.

- The SEM results showed that annealing operation eliminates the effect of the layered structure and minimizes the effect of the printing pattern on the mechanical properties and shape memory effect. As a result, the fiber-polymer interface was strengthened and the

22

internal voids and porosity were almost disappeared. This occasion will affect the

mechanical properties of the composite. Also, the higher infill density leads to the

participation of a higher volume of materials in the recovery stage, and a higher recovery

stress was achieved.

References

[1]   Yang S, Zhang Y, Sha Z, Huang Z, Wang H, Wang F, et al. Deterministic Manipulation of
        Heat Flow via Three-Dimensional-Printed Thermal Meta-Materials for Multiple Protection
        of Critical Components. ACS Appl Mater Interfaces 2022.
        doi:10.1021/ACSAMI.2C09602/SUPPL_FILE/AM2C09602_SI_001.PDF.

[2]   Ghanavati R, Naffakh-Moosavy H, Moradi M. Additive manufacturing of thin-walled
        SS316L-IN718 functionally graded materials by direct laser metal deposition. J Mater Res
        Technol 2021;15:2673–85.

[3]   Xiao C, Zheng K, Chen S, Li N, Shang X, Wang F, et al. Additive manufacturing of high
        solid content lunar regolith simulant paste based on vat photopolymerization and the effect
        of water addition on paste retention properties. Addit Manuf 2023;71:103607.
        doi:10.1016/J.ADDMA.2023.103607.

[4]   Jayanth N, Jaswanthraj K, Sandeep S, Mallaya NH, Siddharth SR. Effect of heat treatment
        on mechanical properties of 3D printed PLA. J Mech Behav Biomed Mater
        2021;123:104764. doi:10.1016/J.JMBBM.2021.104764.

[5]   Zhang H, Liu D, Huang T, Hu Q, Lammer H. Three-Dimensional Printing of Continuous
        Flax Fiber-Reinforced Thermoplastic Composites by Five-Axis Machine. Mater 2020, Vol
        13, Page 1678 2020;13:1678. doi:10.3390/MA13071678.

[6]   Sadegh Ebrahimi M, Noruzi M, Hamzehei R, Etemadi E, Hashemi R. Revolutionary auxetic
        intravascular medical stents for angioplasty applications. Mater Des 2023;235:112393.
        doi:10.1016/J.MATDES.2023.112393.

[7]   Bhandari S, Lopez-Anido RA, Gardner DJ. Enhancing the interlayer tensile strength of 3D
        printed short carbon fiber reinforced PETG and PLA composites via annealing. Addit
        Manuf 2019;30. doi:10.1016/j.addma.2019.100922.

[8]   Srinidhi MS, Soundararajan R, Satishkumar KS, Suresh S. Enhancing the FDM infill pattern
        outcomes of mechanical behavior for as-built and annealed PETG and CFPETG composites
        parts. Mater Today Proc 2021;45:7208–12. doi:10.1016/J.MATPR.2021.02.417.

[9]   Hart KR, Dunn RM, Wetzel ED. Increased fracture toughness of additively manufactured
        semi-crystalline thermoplastics via thermal annealing. Polymer (Guildf) 2020;211:123091.
        doi:10.1016/J.POLYMER.2020.123091.

[10]   Abbaslou M, Hashemi R, Etemadi E. Novel hybrid 3D-printed auxetic vascular stent based
        on re-entrant and meta-trichiral unit cells: Finite element simulation with experimental

verifications. Mater Today Commun 2023;35:105742. doi:10.1016/J.MTCOMM.2023.105742.

[11] Aberoumand M, Soltanmohammadi K, Soleyman E, Rahmatabadi D, Ghasemi I, Baniassadi M, et al. A comprehensive experimental investigation on 4D printing of PET-G under bending. J Mater Res Technol 2022;18:2552–69. doi:10.1016/J.JMRT.2022.03.121.

[12] Zapciu A, Amza CG, Baciu F, Vasile MI. Heat treatment of 3D printed polyethylene terephthalate glycol in a supporting powder bed. IOP Conf Ser Mater Sci Eng 2021;1182:012083. doi:10.1088/1757-899X/1182/1/012083.

[13] Soleyman E, Aberoumand M, Rahmatabadi D, Soltanmohammadi K, Ghasemi I, Baniassadi M, et al. Assessment of controllable shape transformation, potential applications, and tensile shape memory properties of 3D printed PETG. J Mater Res Technol 2022;18:4201–15. doi:10.1016/J.JMRT.2022.04.076.

[14] Chalgham A, Ehrmann A, Wickenkamp I. Mechanical Properties of FDM Printed PLA Parts before and after Thermal Treatment. Polym 2021, Vol 13, Page 1239 2021;13:1239. doi:10.3390/POLYM13081239.

[15] Aberoumand M, Soltanmohammadi K, Rahmatabadi D, Soleyman E, Ghasemi I, Baniassadi M, et al. 4D Printing of Polyvinyl Chloride (PVC): A Detailed Analysis of Microstructure, Programming, and Shape Memory Performance. Macromol Mater Eng 2023;308:2200677. doi:10.1002/mame.202200677.

[16] Dai L, Tian C, Xiao R. Modeling the thermo-mechanical behavior and constrained recovery performance of cold-programmed amorphous shape-memory polymers. Int J Plast 2020;127:102654. doi:10.1016/J.IJPLAS.2019.102654.

[17] Feng X, Li G. High-temperature shape memory photopolymer with intrinsic flame retardancy and record-high recovery stress. Appl Mater Today 2021;23:101056. doi:10.1016/J.APMT.2021.101056.

[18] Miaudet P, Derré A, Maugey M, Zakri C, Piccione PM, Inoubli R, et al. Shape and temperature memory of nanocomposites with broadened glass transition. Science (80-) 2007;318:1294–6. doi:10.1126/science.1145593.

[19] Yang Hua, Fei Li, Ning Hu S-YF. Frictional characteristics of graphene oxide-modified continuous glass fiber reinforced epoxy composite. Compos Sci Technol 2022;223:109446. doi:doi.org/10.1016/j.compscitech.2022.109446.

[20] Armin Karimi, Davood Rahmatabadii MB. Various FDM Mechanisms Used in the Fabrication of Continuous-Fiber Reinforced Composites: A Review. Polymer (Guildf) 2024;16:831. doi:https://doi.org/10.3390/polym16060831.

[21] Mohammadizadeh M, Imeri A, Fidan I, Elkelany M. 3D printed fiber reinforced polymer composites - Structural analysis. Compos Part B Eng 2019;175:107112. doi:10.1016/J.COMPOSITESB.2019.107112.

[22] Tekinalp HL, Kunc V, Velez-Garcia GM, Duty CE, Love LJ, Naskar AK, et al. Highly oriented carbon fiber–polymer composites via additive manufacturing. Compos Sci Technol 2014;105:144–50. doi:10.1016/J.COMPSCITECH.2014.10.009.

[23] Arash B, Park HS, Rabczuk T. Tensile fracture behavior of short carbon nanotube reinforced polymer composites: A coarse-grained model. Compos Struct 2015;134:981–8. doi:10.1016/J.COMPSTRUCT.2015.09.001.

[24] Kumar KS, Soundararajan R, Shanthosh G, Saravanakumar P, Ratteesh M. Augmenting effect of infill density and annealing on mechanical properties of PETG and CFPETG composites fabricated by FDM. Mater Today Proc 2021;45:2186–91. doi:10.1016/J.MATPR.2020.10.078.

[25] Popescu D, Zapciu A, Amza C, Baciu F, Marinescu R. FDM process parameters influence over the mechanical properties of polymer specimens: A review. Polym Test 2018;69:157–66. doi:10.1016/j.polymertesting.2018.05.020.

[26] Syrlybayev D, Zharylkassyn B, Seisekulova A, Akhmetov M, Perveen A, Talamona D. Optimisation of Strength Properties of FDM Printed Parts—A Critical Review. Polym 2021, Vol 13, Page 1587 2021;13:1587. doi:10.3390/POLYM13101587.

[27] Shbanah M, Jordanov M, Nyikes Z, Tóth L, Kovács TA. The Effect of Heat Treatment on a 3D-Printed PLA Polymer's Mechanical Properties. Polym 2023, Vol 15, Page 1587 2023;15:1587. doi:10.3390/POLYM15061587.

[28] Koske D, Ehrmann A. Advanced infill designs for 3d printed shape-memory components. Micromachines 2021;12:1225. doi:10.3390/mi12101225.

[29] Peng Wang BZ. Improvement of Heat Treatment Process on Mechanical Properties of FDM 3D-Printed Short- and Continuous-Fiber-Reinforced PEEK Composites. Coatings 2022;12:827. doi:https://doi.org/10.3390/coatings12060827.

[30] Seok W, Jeon E, Kim Y. Effects of Annealing for Strength Enhancement of FDM 3D-Printed ABS Reinforced with Recycled Carbon Fiber. Polym 2023, Vol 15, Page 3110 2023;15:3110. doi:10.3390/POLYM15143110.

[31] Rahmatabadi D, Soltanmohammadi K, Aberoumand M, Soleyman E, Ghasemi I, Baniassadi M, et al. 4D printing of porous PLA-TPU structures: effect of applied deformation, loading mode and infill pattern on the shape memory performance. Phys Scr 2024;99:025013. doi:10.1088/1402-4896/AD1957.

[32] Ghorbani J, Koirala P, Shen Y-L, Tehrani M. Eliminating voids and reducing mechanical anisotropy in fused filament fabrication parts by adjusting the filament extrusion rate. J Manuf Process 2022;80:651–8. doi:10.1016/J.JMAPRO.2022.06.026.

[33] Tao Y, Kong F, Li Z, Zhang J, Zhao X, Yin Q, et al. A review on voids of 3D printed parts by fused filament fabrication. J Mater Res Technol 2021;15:4860–79. doi:10.1016/J.JMRT.2021.10.108.